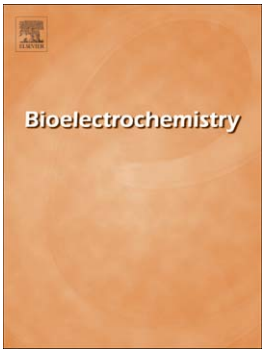

Synthesis of one-dimensional gold nanostructures and the electrochemical application of the nanohybrid containing functionalized graphene oxide for cholesterol biosensing

Seetharamaiah Nandini, Seetharamaiah Nalini, M.B. Madhusudana Reddy, Gurukar Shivappa Suresh, Jose Savio Melo, Pathappa Niranjana, Jakkid Sanetuntikul, Sangaraju Shanmugam

PII: S1567-5394(16)30040-8
DOI: doi: 10.1016/j.bioelechem.2016.03.006
Reference: BIOJEC 6933

To appear in: *Bioelectrochemistry*

Received date: 7 November 2015
Revised date: 25 March 2016
Accepted date: 26 March 2016

Please cite this article as: Seetharamaiah Nandini, Seetharamaiah Nalini, M.B. Madhusudana Reddy, Gurukar Shivappa Suresh, Jose Savio Melo, Pathappa Niranjana, Jakkid Sanetuntikul, Sangaraju Shanmugam, Synthesis of one-dimensional gold nanostructures and the electrochemical application of the nanohybrid containing functionalized graphene oxide for cholesterol biosensing, *Bioelectrochemistry* (2016), doi: 10.1016/j.bioelechem.2016.03.006

Synthesis of one-dimensional gold nanostructures and the electrochemical application of the nanohybrid containing functionalized graphene oxide for cholesterol biosensing

Seetharamaiah Nandini[a,d], Seetharamaiah Nalini[a,d], M. B. Madhusudana Reddy[b], Gurukar Shivappa Suresh[a,*], Jose Savio Melo[c,*], Pathappa Niranjana[d,*], Jakkid Sanetuntikul[e], Sangaraju Shanmugam[e]

[a]*Department of Chemistry and Research Centre, N.M.K.R.V. College for Women, Jayanagar, Bangalore 560 011, India*

[b]*School of Chemistry, Reva University, Kattigenahalli, Yelahanka, Bangalore 560064, India*

[c]*Nuclear Agriculture and Biotechnology Division, Bhabha Atomic Research Centre, Mumbai 400 085, India*

[d]*Department of PG Studies and Research in Biochemistry, Jnana Sahyadri, Kuvempu University, Shankarghatta, Shimoga 577451, India*

[e]*Department of Energy Systems and Engineering, Daegu Gyeongbuk Institute of Science and Technology, Daegu 711-873, Republic of Korea*

**Corresponding authors*
Telephone: 91-80-26654920
Fax no: 91-80-22453665
E-mail: sureshssmrv@yahoo.co.in (G.S. Suresh),
jsmelo@barc.gov.in (J.S. Melo) and
bpniru@gmail.com (P. Niranjana)

Abstract

This manuscript reports a new approach for the synthesis of one dimensional gold nanostructure (AuNs) and its application in the development of cholesterol biosensor. Au nanostructures have been synthesized by exploiting β-diphenylalanine (β-FF) as an sacrificial template, whereas the Au nanoparticles (AuNPs) were synthesized by ultrasound irradiation. X-ray diffractometer (XRD), scanning electron microscope (SEM) and energy dispersive analysis of X-rays (EDAX) have been employed to characterise the morphology and composition of the prepared samples. With the aim to develop a highly sensitive cholesterol biosensor, cholesterol oxidase (ChOx) was immobilized on AuNs which were appended on the graphite (Gr) electrode via chemisorption onto thiol-functionalized graphene oxide (GO-SH). This Gr/GO-SH/AuNs/ChOx biosensor has been characterized using cyclic voltammetry (CV), electrochemical impedance spectroscopy and chronoamperometry. CV results indicated a direct electron transfer between the enzyme and the electrode surface. A new potentiostat intermitant titration technique (PITT) has been studied to determine the diffusion coefficient and maxima potential value. The proposed biosensor showed rapid response, high sensitivity, wide linear range and low detection limit. Furthermore, our AuNs modified electrode showed excellent selectivity, repeatability, reproducibility and long term stability. The proposed electrode has also been used successfully to determine cholesterol in serum samples.

Keywords: gold nanostrucutres, functionalized graphene oxide, electrochemical biosensor, β-diphenylalanine, peptide nanotubes, cholesterol

1. Introduction

Cardiovascular diseases are a cause for high mortality rate and rank as the second highest in the list of deadliest diseases. It is caused by many factors but the most common is atherosclerosis which is characterized by thickening of arteries due to the deposition of cholesterol in its inner walls. Cholesterol, a waxy sterol is an essential structural component of nerve cells, brain cells, plasma membrane and are precursors of biological materials such as hormones, vitamin D, etc [1]. However, having a high or low level of cholesterol may be correlated to a number of clinical disorders [2]. Consequently, regular assessment of cholesterol has been the subject of a plethora of investigations in clinical diagnostics. Classically, several well-known analytical methods like HPLC, colorimetric, spectrophotometric have been developed for the quantification of cholesterol [3]. However, the limitations of these traditional methods are time consumption and cumbersome procedures. As an alternative tool for measurement, many researchers are relying on developing electrochemical methods. Ideally, electrochemical biosensors are efficient, inexpensive, accurate, sensitive, rapid and offer objective information. In principle, these electrochemical biosensors are dependent on the immobilization of cholesterol oxidase (ChOx) onto the electrode surface. ChOx (EC 1.1.3.6) is a 56 kDa protein incorporating Flavin Adenine Dinucleotide (FAD) as co-factor in the active site which catalyzes the oxidation of cholesterol by molecular oxygen to 4-cholesten-3one [4]. However, the critical challenge in the fabrication of ChOx based biosensors is a reliable enzyme immobilization procedure considering the deep embedding of the active centre in the protein making it difficult for the electron to transfer between the enzyme and the electrode. Concurrently, great efforts have been devoted to establish a foundation for the ease of electron transfer by incorporating novel electrode materials in the fabrication of biosensor. The adoption of nano-structured materials can endow high effective surface area for enhanced enzyme loading, biocompatibility and offer high electron communication characteristics with elevated sensitivity.

In the past decades, intense fundamental and technological advances have placed a prime focus on nanoparticle research due to their potential applications in catalysis, nanoelectronics, sensors, etc [5,6]. In the nanoscale reign, literature reveals many methods [7,8] for the preparation of metal nanoparticles with well controlled geometrical parameters such as size and shape. Subsequently experimental results have suggested advanced nanocrystals structures with comprehensive geometries including wires, ribbons, belts and other structural morphologies [9,10]. During the past decade, rapid advancement in the nanoparticle synthesis has laid an important landmark in the development of inorganic tubular/hollow nanostructures whose attractiveness emerges from their catalytic activities, lofty surface area and large porosity [11,12]. The preparation of inorganic hollow nanostructures composed of desirous metal nanoparticles as building blocks in their tube walls has stimulated fascinating research interest in material scientists. These one dimensional metal nanostructures are known to possess unique physical and chemical properties unlike their solid counter-parts with dominance of enhanced catalyst loading ensuing intensified electron transfer kinetics. A variety of metal nanostructures [13,14] have been fabricated successfully by several research groups. However there is a compelling evidence for the fabrication of one dimensional Au nanostructures (1D AuNs) with catalytic applications, owing to their high conductivity, biocompatibility, resistance to oxidation and sensitivity [15]. In view of this paramount importance, some researchers have demonstrated that 1D AuNs can be prepared by template synthesis using hard templates, soft templates and sacrificial templates [16-18]. Besides, Reches and Gazit have proposed a versatile method of peptide-based template directed synthesis of silver nanotubes [19]. On account of their intriguing properties like crystallinity, temperature and pH stability, biocompatibility, chemical diversity and so forth peptide-based

templates are speculated to be a promising candidate for fabricating metal nanostructures [20]. This has paved way for concerted research work on peptide as self assembling biotemplate for fabricating Au nanowires [21] coaxial metal nanocables [22] peptide nanotubes Pt nanocomposites [23] etc., Furthermore, scrupulous placement of AuNs onto the electrode is of practical importance in-order to beneficently take the advantages of their outstanding properties. This can be achieved by chemical derivatization of underlying substrate by linking the nanotubes with the functional groups like thiol, amine, etc., present on the substrate.

Graphene is a two-dimensional honey comb like nanostructure, composed of monolayer of sp^2 hybridized carbon atoms. The excellent prospectus of graphene such as high surface area for molecular adsorption, fast electron transportation, high conductivity, easy functionalization, admirable dispersibility in aqueous solvent [24] etc., permits its use as an excellent substrate for dispersion of metal nanoparticles. However, chemical derivatization of graphene is necessitous to expand the horizons of its applications. In particular, oxygen derivatized candidate graphene oxide has come into the limelight of graphene-metal nanoparticle composites owing to the presence of residual oxygen-containing functional groups which permit easier chemical functionalization. Hitherto, several researchers have testified the synergy, exceptional stability of these graphene-metal nanocomposites in biosensors. Accordingly, the graphene-oxide with thiol functionalization can bestow chemically active sites for anchoring Au nanostructures by enhancing their stability and the resulting hybrid nanostructures can exhibit crucial properties like exceptional stability, low detection limit, high sensitivity and synergy.

Herein, we describe an efficient method for the fabrication of electrochemical cholesterol biosensor which was constructed by utilizing the beneficial properties of AuNs and thiol-functionalized graphene oxide (GO-SH). In the current work, the preparative protocol for AuNs begins with the hierarchical assembly of AuNPs to form 1D nanostructures employing conformationally flexible β-diphenylalanine peptide nanotubes (β-FFNTs) as a template and the concomitant formation of ordered Au nanostructures through proteolytic cleavage of the template. For this purpose, AuNPs was synthesized by ultrasonic irradiation. Although there are ample reports on the self assembly of FF (composed of α- amino acids) into tubular ensembles [20-23], we sought to exploit the appealing features of peptide by using β-amino acids for the first time as it has been appraised that β peptides can form stable and flexible conformation as compared to the α-peptides [25]. To the best of our knowledge, this is the first report on β dipehnylalanine (β –FF) using β peptides that has been successfully employed to adopt tubular constructs that consecutively served as template for the synthesis of well-defined 1D AuNs. In addition, we have also demonstrated the electrocatalytical properties of these Au nanostrucutres towards cholesterol detection. With the aim of improving the long-term binding affinity of AuNs onto the graphite electrode (Gr) throughout the electrochemical experiments, the surface of Gr was modified with GO-SH. The structural and qualitative analysis of the nanocomposite has been investigated using XRD, SEM and EDAX. Furthermore, cholesterol biosensor was fabricated by drop casting ChOx on nanohybrid composite as an immobilization scaffold and we examined the electrocatalytic activity of the Gr/GO-SH/AuNs/ChOx modified electrode towards cholesterol estimation by using CV and Chronoamperometry. The proposed biosensor was evaluated in terms of thermal stability, effect of pH, optimum working potential, influence of electroactive species and electrochemical stability. Finally the reproducibility and repeatability of the biosensor was also studied. We believe that the GO-SH/AuNs nanohybrid composite offers a novel prospective such as enhanced enzyme loading, high sensitivity as validated from the experimental results.

2. Experimental section

2.1. Reagents and materials

Gold (III) chloride hydrate ($HAuCl_4$), cholesterol, proteinase K, ascorbic acid (AA),uric acid (UA), dopamine (DA), triton X, isopropanol, (3-Mercaptopropyl) trimethoxysilane (MPTMS), *N*,*N*'-dicyclohexylcarbodiimide (DCC), sodium dodecyl sulphate (SDS) and sodium perchlorate ($NaClO_4$) were purchased from Sigma Aldrich. 1,1,1,3,3,3-hexafluoro-2-propanol (HFIP), Di-tert-Butylpyrocarbonate (Boc), triethylamine, methanol, ethylacetate, and thionyl chloride were procured from Spectrochem Pvt. Ltd, India. L-Phenylalanine was obtained from Loba Chemie. Chemical derivatization of Gr with thiol functional group for chemisorptions was achieved by two synthetic procedures [26]. In typical experimental protocol, Gr was first converted to Graphite oxide according to Hummer's method. Consequently, the graphite oxide was dissolved in dichloromethane with the aid of ultrasonication. To this dispersion, MPTMS was added at a concentration of 2 mg/mL and refluxed at 70 °C for 12 hrs. This resulted in thiol functionalized graphene oxide (GO-SH). The so obtained product was washed with tetrahydrofuran and ethanol several times and finally dried at 60 °C for overnight time period under vacuum. 30 % H_2O_2, dichloromethane, thionyl chloride were purchased from Merck Ltd., while ChOx (500 U/mg) was procured from SRL, India. Prior to modification, the surface of the Gr electrode was well polished mechanically to mirror finish with 0.05 mm aqueous polishing alumina and sequentially with 1 mm polishing diamond using PK-3 electrode polishing kit (BAS Inc. Tokyo, Japan). The supporting electrolyte used was 0.1 M phosphate buffer solution (PBS) prepared by mixing the stock solutions of 0.1 M K_2HPO_4 and 0.1 M KH_2PO_4 and the pH was adjusted using NaOH and HCl. All the chemicals unless and otherwise mentioned in this investigation are of analytical grade.

2.2. Apparatus

All the electrochemical measurements were recorded using standard single compartment of three-electrode configuration with Platinum foil as a counter electrode, saturated calomel as the reference electrode (SCE) and Gr or ChOx modified as working electrode. Morphological characterization and the compositional investigation were assessed by scanning electron microscope (SEM) and energy dispersive analysis of X-rays (EDAX) respectively using FE-SEM; model Hitachi S-4800 II with an accelerating voltage of 5 kV. Powder X-ray diffraction patterns were obtained with an XRD benchtop powder diffraction system using Cu Kα radiation as a source (λ= 0.15443 nm, Proto Manufacturing Inc). Ultrasonic irradiation was achieved with 20 kHz acoustic waves generated by a titanium horn (Q Sonica Ultrasonic processor).The electrochemical characteristics examined by cyclic voltammetry (CV), chronoamperometry and electrochemical impedance spectroscopy (EIS) were performed by employing computer controlled electrochemical analyzer (Versa stat 3, Princeton Applied Research, USA). The EIS study has been carried out with AC voltage amplitude of 5 mV in the frequency range 0.1 to 100 kHz and fitting of experimental spectroscopy data to the equivalent circuit was done by means of software "Zsimp Win" version 3.20. Prior to electrochemical measurements the electrolyte was saturated with pure oxygen at ambient conditions.

2.3. Synthesis of AuNPs, β-FF, β-FFNTs and AuNs

AuNPs was synthesized using ultrasound irradiation following the reported experimental procedures with slight modification. Briefly, 250 mL of 0.05 g $HAuCl_4$ solution as metal

precursor containing 0.05 M isopropanol as radical scavenger was purged with argon for 20 min. To this solution, 0.01 M SDS as surfactant and 0.01 M $NaClO_4$ as electrolyte were added and ultrasonic irradiation was performed at a frequency of 20 kHz. The colour of the solution changed from yellow to black and to red wine indicating the reduction of $HAuCl_4$ ions into AuNPs. The red wine solution of AuNPs was preserved for the synthesis of AuNs and it was found to be stable for several weeks at room temperature (25-30°C) whereas the storage stability can be prolonged for three months when refrigerated (4°C) and properly stored in a dark brown bottle.

The β-FF was prepared using conventional solution-phase methodology. The N-terminus of first α-amino acid and C- terminus of the second α-amino acid were protected by Boc and methylester (OMe) respectively [27]. Basically, as demonstrated by Seebach *et al*. homologation of Boc and OMe protected α-amino acid was carried out following Arndt-Eistert reaction [28]. Subsequential coupling reaction was accomplished using DCC as a coupling reagent. The crude peptide obtained was isolated using HPLC and the identity of the β-FF was confirmed by mass spectroscopy. The diphenylalanine peptide nanotubes were synthesized following Reches and Gazit method [19]. Briefly, as synthesized β-FF was dissolved in HFIP at concentration of 100 mg/mL which on further dilution with water at a concentration of 2 mg/mL results in the formation of peptide nanotubes.

Finally, the synthesis of AuNs was accomplished by mixing the as prepared colloidal AuNPs solution with peptide nanotubes solution in the concentration ratio of 4:1 respectively [22]. This ratio was optimized by conducting a series of experimental procedure by varying the AuNPs for each mixture while maintaining the concentration of peptide constant. After overnight incubation at 4 °C, a red-wine precipitate was obtained at the bottom of the glass beaker indicating AuNPs bunched on the peptide nanotubes. The final solid product was recovered by centrifugation, thoroughly washed with water, dried in vacuum at 65 °C for 7 hr and ultimately subjected to proteolytic cleavage using proteinase K at concentration of 100 µg/mL [19] and incubated at 35 °C for 1 hr to form AuNs. The resultant solid mass was suspended in water for the modification of the electrode. The as synthesized AuNs exhibited long term stability for 6 months when stored at RT and if stored at low temperature (4°C), it is stable for at least 9 months.

2.4. Fabrication of cholesterol biosensor

Gr rod of geometric surface area of 0.28 cm^2 (diameter *ca* 6 mm) was mounted into a custom-made Teflon compartment having same internal diameter. Electrical connectivity was established using a Cu wire. A schematic illustration of fabrication of the electrode is given in Scheme-1. The Gr surface was polished repeatedly using alumina and diamond slurry, washed successively using ultrasonic agitation in water and dried. The desired thiol modification for strong adhesion of 1D AuNs was achieved by coating 10 µL aliquot of homogenous suspension of ultrasonically dispersed GO-SH, which provides necessary support to anchor AuNs and facilitates conduction of electrons. This coating was allowed to dry at ambient temperature for 1 hour. After complete drying, 10 µL of AuNs (10 mg/mL) was cast on the underlying SH substrate, followed by 2 hr of drying at RT. Then 10 µL of ChOx was pipetted and uniformly spread on the surface for covalent binding between enzyme and the AuNs. Then, the enzyme modified electrode was dried at 4 °C for 1 hr and rinsed with water to remove any unbound ChOx. Prepared electrode was designated as Gr/GO-SH/AuNs/ChOx. To compare the electrochemical performance with respect to cholesterol determination three more electrodes denoted as Gr/ChOx, Gr/GO-SH/ChOx and Gr/GO-SH/AuNs were also prepared in similar manner.

3. Results and Discussion

3.1 Structural characterization using XRD

To gain an insight into structural investigation and phase identification, XRD patterns of AuNPs, β-FFNTs and nanotubes templated AuNPs binding (AuNPs@ β-FFNTs) were obtained and are depicted in Fig. 1 (A-C). The Fig. 1A corresponds to the XRD data of AuNPs prepared by ultrasonic irradiation. It can be clearly observed that strong and sharp peaks at the positions of $2\theta = 38.1°$, 44.1° and 64.6° is related to the characteristic diffraction peaks of Au element demonstrating that as synthesized AuNPs resembles a face-centred cubic structure oriented in (111), (200) and (220) directions without any impurity phase. The diffraction pattern for β-FFNTs (B) was also measured for comparison. The XRD peaks at 2θ=10.03°, 18.3°, 19.6° positions resemble those of the peptide nanotubes reported in the literature [29]. However, it is interesting to note that the similar trend of XRD pattern was replicated for AuNPs@ β-FFNTs (C) indicating the co-existence of very weak reflections corresponding to metallic fcc phase of AuNPs along with dominant reflections corresponding to β-FFNTs. Considering this XRD result we assume that AuNPs ensemble selectively to the β-FFNTs structures. In addition, there exist perceptible differences between these XRD patterns: which is in the positive shift in the position of reflection peak as compared to both (A) and (B) which further suggest the idea that the AuNPs has been incorporated in the β-FFNTs lattice. Our data as shown in the Fig.1 were found to correlate with the XRD results as reported for FFNTs and AuNPs. The calculated average crystalline size of AuNPs is found to be 13.8 nm as estimated from the width at half height of most intense diffraction line by Scherer's equation.

3.2. Physical characterization of the modified electrodes using SEM and EDAX

The morphology of the AuNPs, self assembled peptide nanotubes, AuNPs templated peptide nanotubes and AuNs obtained as a resultant of proteolytic peptide cleavage were determined by SEM measurements. Fig.2 illustrates the representative SEM images as evaluated for these four samples. The micrograph of AuNPs (panel 'A') exhibits highly disperse bright colour spherical particles with minimal or no aggregation. Statistical analysis of the particle size distribution obtained using ImageJ software (NIH) is illustrated in panel 'B'. From the corresponding histogram results, the average particle diameter of AuNPs was calculated to be 14 ± 2.85 nm with a size distribution standard deviation (σ) of 2.85 nm and polydispersity ($xc/\sigma \times 100$) ≈ 20%. Interestingly, the self assembled β-FF (panel C) shows smooth, straight, elongated individual entities with 80-100 nm in diameter and μm lengths. The different lengths of tubes can be presumed to be due to the experimental conditions that could have fragmented the long tubular peptide nanostructures ensuing smaller length nanotubes. A highly magnified SEM image in the inset of panel 'C' represents a single peptide nanostructure with tubular hollow interior which clarifies the formation of peptide nanotubes from β-FF. However upon increased dilution of the peptides with water at concentration of 1 mg/mL a change of morphology is evident. It is obvious from the Fig. 2D that the peptides self assembled into hollow microstructures due to increased hydrophobic content. In the corresponding high-magnification SEM image (Fig. 2D Inset), presence of numerous nanofibers can be clearly observed indicating the impressive alignment of these fibres into a nest-like microstructures. Surprisingly, the AuNPs templated peptide nanotubes [Fig. 2E] demonstrate preferential growth of bright spherical shaped blisters along the tubular direction of the template. This provides basis of the assumption of binding of AuNPs to the peptide template via electrostatic interactions. It appears from the Figure, that the particle size of these connected grains is ≥ 25 nm in diameter suggesting that the enwrapped peptide nanotubes might have multiple metal nanoparticles to obstruct the pores of the template for added AuNPs. Nevertheless, this can be avoided by using low concentration of metal

nanoparticles. For further comparison, a SEM measurement was carried out following peptide cleavage and was examined. According to the image analysis of panel 'F', the proteolytic cleavage eliminated most of the peptide nanotubes and remarkable hollow end of the tubular morphology is also seen as indicated by the arrow. Besides, we can notice an individual entity of single 1D AuNs in the inset of Fig.2F revealing that the 1D metal nanostructures have not only the feature of the template but also have same diameter size than the peptide nanotubes. These data validates that the peptide nanotubes are effective to be used as template for the synthesis of one dimensional metal nanostructure. Subsequently, EDAX was employed to provide qualitative information of the elements and the contents of the as prepared nanostructures. Typical EDAX of these four samples is given in supporting information.

3.3. Electrochemical characterization of the bioelectrode using CV and EIS using potassium ferricyanide

The electrochemical characterization after each surface modification of the electrode were investigated by CV and EIS in 5 mM $Fe(CN)_6^{3-/4-}$ (1:1) mixture as a redox probe in 0.1 M PBS. As seen in Fig. 3A the curve of bare Gr (a) showed a redox peak with an anodic peak potential at 0.318 V and a cathodic peak potential at 0.124 V which has a peak separation of 194 mV. Compared to curve (a), the curve (b) of thiol functionalized graphene oxide exhibited a lower peak current with higher peak separation of 212 mV, this may be attributed to the presence of thiol groups which in turn obstruct the acquiesce of ferrocene ions resulting in current plummet [30]. From curve c (Gr/GO-SH/AuNs), it can be observed that the peak currents were much larger which can be assigned to preoccupy of Au to the thiol groups indicating the strong binding of metal nanoparticles rendered by the chemically derivatized GO-SH. In contrast, the enzyme modified electrode (curve d) showed lower peak currents for the electrochemical redox probe indicating that ChOx had been successfully immobilized on the surface of the Gr/GO-SH/AuNs electrode. This can be ascribed to enzyme that acts as an insulator leading to the repulsion of ferrocene ions $Fe(CN)_6^{3-/4-}$

Electrochemical impedance spectroscopy (EIS) is a widely used effectual and fast technique to measure the electrical properties of materials and their interfaces with electron conducting electrodes [31]. The EIS measurements for the different electrodes were conducted and the results are as shown in Fig. 5B. The semi circle part corresponds to high frequency impedance, where as the linear part associates to the diffusion step of the overall processes. As shown in inset of Fig. 5B, the Randle's equivalent circuit was initiated to fit satisfactorily the data as given in Table 1 obtained over the measured frequency range. The circuit is composed of R_s – the ohmic resistance of the electrolyte solution, R_{ct} is the electron transfer resistance, R_f– film resistance, Q_1 is the constant phase element related to the charge capacitance at the electrode/electrolyte interface, Q_2 is the constant phase element related to the charge capacitance at the metal/electrolyte interface and W is the Warburg impedance due to mass transfer to the electrode surface. The Gr/GO-SH/AuNs/ChOx electrode displayed a large semi circle representing a high electron transfer resistance of ferrocene ions by the ChOx film. This may be attributed to the poor electron conductivity of ChOx enzyme. On the contrary, Gr/GO-SH exhibited a semicircle with small diameter than Gr/GO-SH/AuNs/ChOx and a large diameter contrast to bare Gr attributed to the large electron transfer resistance which is higher than that of the bare Gr. Whereas, Gr/GO-SH/AuNs exhibited a smallest semicircle indicating a lower electron transfer resistance due to the better electrical conductivity property of AuNs. As evident from the table, the electron transfer resistance (R_{ct}) shows an increase after each electrode modification process except for the Gr/GO-SH/AuNs electrode. As mentioned earlier, R_{ct} is the resistance which controlled the transfer of the redox probe through the electrode surface. The Gr/GO-SH/AuNs had better

conductivity than the other modified electrode due to which a decreased R_{ct} value was obtained. In contrast, the R_{ct} of Gr/GO-SH was notably increased in comparison with the bare Gr which can be attributed to the electrostatic interaction between thiol group and ferrocene ions [30]. In addition, the Gr/GO-SH/AuNs/ChOx electrode exhibited a larger R_{ct} value due to the resistance of ferocene ions by the ChOx immobilized on the electrode surface. The change in the passive layer of the each modified electrode is represented by Q_1 and Q_2. It is apparent that the Q_1 value is more for the Gr/GO-SH/AuNs electrode which may be attributed to the increased surface area of the electrode and the excellent electroconducting properties of the AuNs. The bare Gr exhibited a Q_1 value more compared to the Gr/GO-SH and Gr/GO-SH/AuNs/ChOx modified electrodes because of the occurrence of carbon groups in the Gr surface. Whereas, the Gr/GO-SH electrode exhibited lesser Q_1 value owing to the carbon groups that has been engaged by thiol groups. Similarly, the Gr/GO-SH/AuNs/ChOx displayed a least Q_1 value because of the presence of non-conducting capacity of ChOx enzyme. Furthermore, the '*n*' values for the electrodes fluctuate between 0.8 to 1 indicating the homogenous porosity nature of the electrode surface. The extremely sluggish progression in the bulk of the composite film on the electrode surface is given by constant phase element Q_2 (with the exponent *n*2) [32]. The Q_2 and R_{ct} relates to the processes taking place at lower frequencies whereas Q_1 and R_f relates to the processes occurring at higher frequencies. Higher the Q_2 value, higher the diffusion of ferrocene ions. However, an increase in R_f suggests that the ferrocene ions diffuse and accumulate into the electrode surface and lower R_f indicates the resistance of the ferrocene ions by the electrode surface. The Warburg response in an EIS study is expected due to the thickness of the diffusion layer on electrode surface and its inability to allow ferrocene ions. The lower W value in the present investigation indicates that the surface layer is thinner which can allow the ions to pass through it. From these experimental results, it can be inferred that there exists an excellent relationship between semicircle diameters and electrode layers, which signify successful construction of the biosensor.

3.4. Comparison of the voltammetric response of the modified electrodes towards cholesterol detection

In order to describe the enhanced performance of the (d) Gr/GO-SH/AuNs/ChOx electrode towards cholesterol detection, we investigated the CVs of (a) Gr/ChOx (b) Gr/GO-SH/ChOx and (c) Gr/GO-SH/AuNs in presence of 0.3 mM cholesterol recorded under similar experimental conditions. Fig. 4 demonstrates the so obtained results probed in oxygen saturated 0.1 M PBS in the potential range 0 to −0.75 V at a scan rate of 50 mV/s. It is clearly seen that the current density associated with the cholesterol detection for curve 'a' is very low illustrating that Gr alone in inactive for the electrocatalytic reduction of cholesterol. Under comparable conditions, the Gr/GO-SH/ChOx modified electrode showed an increased peak current with virtually no oxidation or reduction peak implying an enhanced electrochemical activity of the electrode due to the incorporation of GO-SH. In addition, we also attempted to probe the electron conductivity of AuNs (b') over AuNPs (a') modified electrode by CV measurements as summarized in the Inset of Fig. 4. Evidently, the AuNs modified electrode showed good electron conductivity which is three times higher than AuNPs solely incorporated electrode. While the voltammetry of Gr/GO-SH/AuNs modified electrode (curve c) for cholesterol detection showed slight increase in peak current ascribed to the increased surface coverage area of the electrode. However, the best electrocatalytic performance was obtained with the proposed biosensor (d) indicating the electrode composite possess the synergistic effects of GO-SH as well as AuNs which provides largest surface to volume ratio thus higher surface activities among the other ChOx modified electrodes used in the present investigation. In addition a new feature of oxidation and reduction peak located at

−0.35 V and −0.450 V corresponding to the FAD/$FADH_2$ active centres of ChOx was observed at the Gr/GO-SH/AuNs/ChOx electrode. Such a characteristic redox peaks with a formal potential of −0.4 V (calculated by averaging the anodic and cathodic peak potentials) can be concurred well with the reported literature [33] attesting that the direct electron transfer from the redox centres of ChOx to the electrode surface and vice versa is accomplished by the biocompatible AuNs and its synergy with GO-SH. This result validates the enhanced electron conductivity of AuNs, successful immobilization of ChOx and the most favourable orientation of the active centres which retain the enzyme's native structure.

3.5 Electrocatalytic properties of the Gr/GO-SH/AuNs/ChOx biosensor

CV was used to study the electrocatalytic behaviour of the Gr/GO-SH/AuNs/ChOx electrode towards increasing concentration of cholesterol. As can be seen in Fig. 5A a pair of well behaved redox peaks appeared at about −0.35 and −0.450 V with a formal potential of about −0.4 V. This peak potential is appraised as a direct electron transfer between the redox active centres of FAD/$FADH_2$ in ChOx and electrode surface at pH 7 [33]. Despite the fact that the CV exhibits a quasi reversible voltammetric response it is still considered as redox electrochemistry, because of the presence of anisotropic GO-SH which exhibits hydrophobicity and ionic character to AuNs. Sequentially, AuNs has an added advantage over Au due to its nanometre size and its tubular shape which afford exorbitant surface area, favoured electronic properties, superior electrocatalytic activity and congenital biocompatibility for the attachment of ChOx enabling electron transfer [34]. The voltammetric responses of the Gr/GO-SH/AuNs/ChOx with the addition of different concentrations of cholesterol ranging from 0−6 mM resulted in gradual increase in anodic peak with concomitant decrease in cathodic peak which may be attributed to the consumption of oxygen by ChOx, leading to the dismissal of hydrogen from C(3)-OH group in cholesterol molecule generating Carbonyl product. In reduction process, the oxidized FAD co-factor admits a hydride from the substrate whereas; during oxidation process the reduced flavin transfers the redox equivalents to molecular oxygen yielding H_2O_2. The carbonyl species can also catalyze the isomerisation of cholest-5-en-3-one to cholest-4-en-one [2]. The enzymatic reaction between cholesterol and ChOx [35] is as shown below:

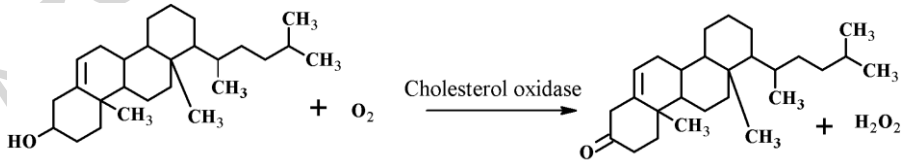

Cholesterol Cholesteone

The effects of scan rate were investigated as illustrated in Fig. 5B. The anodic and peak currents (I_{pa} and I_{pc}) were linearly proportional to the scan rate in the range from 10−100 mV/s suggesting that the electrode reaction is surface controlled process. The linear regression equations for cathodic and anodic peak currents are as follows-

$$I_{pa} = -1.980\times10^{-5}+9.396\times10^{-7}\ \upsilon\ (\text{V/s});\ R= 0.999 \qquad (1)$$

$$I_{pc} = -4.224\times10^{-5}-(-1.081\times10^{-5})\ \upsilon\ (\text{V/s});\ R= -0.997 \qquad (2)$$

The anodic and cathodic peak potentials are linearly dependent on the logarithm of scan rates (υ). When $n\Delta E_p < 200$ mV, the electron transfer rate constant k_s could be calculated according to Laviron's equation [36] as follows-

$$\log k_s = \alpha \log (1-\alpha) + (1-\alpha) \log \alpha - \log RT/nF\upsilon - \alpha (1-\alpha)\, nF\Delta E_p/2.3RT \quad (3)$$

Where α is the electron transfer coefficient, n is the electron transfer number, k_s is apparent heterogeneous electron transfer rate constant, υ is the scan rate, $E^{o'}$ is the apparent formal potential, F- Faraday's constant, R is Gas constant and T is absolute temperature. The electron transfer coefficient was obtained from the slope of the peak potential against the logarithm of the scan rate which was found to be 0.25. From the slope of ΔE_p vs. log υ, the electron transfer coefficient of Gr/GO-SH/AuNs/ChOx was estimated to be 0.096 s^{-1}. This value is greater than ChOx/MWCNTs/GCE [37] (0.0269 s^{-1}) these results suggests that Gr/GO-SH/AuNs/ChOx electrode exhibits fast electron transfer.

3.6 Potentiostatic intermittent titration technique for Gr/GO-SH/AuNs/ChOx electrode

The potentiostatic intermittent titration technique (PITT) has been extensively used in Lithium ion battery (LIB) for the study of lithium diffusion coefficient and thermodynamics of LIBs. The speculations behind this technique are as follows [38]:-

a) The diffusion coefficient is a parameter which occurs due to the diffusion of only one species in the electrochemical system and is persistent solely dependent on the applied potential range.
b) Diffusion takes place in an electrode, within its thinnest dimension of a dense electrode with slab geometry.
c) During the diffusion process, there will be no interfacial reaction resistance at the electrode-electrolyte interface.
d) There is no phase transformation related kinetics

Many manuscripts have reported the calculation of diffusion coefficient using Randle's Sevick equation in EIS. The advantage of PITT over EIS technique is the calculation of the diffusion coefficient lies in the fact that the semi-infinite diffusion region is readily sustained in the $It^{1/2}$ vs. log t plots, moreover the diffusion coefficient obtained by EIS are subjected to errors [39]. In this manuscript we have used PITT in biosensors for the first time to estimate the diffusion coefficient of cholesterol in Gr/GO-SH/AuNs/ChOx electrode. The chronoamperometric response of Gr/GO-SH/AuNs/ChOx electrode towards cholesterol was studied at a potential range from −0.42 V to −0.6 V vs. SCE. Inset of Fig.6A, shows $It^{1/2}$ vs. log t plots in the potential range studied with the highest values of $It^{1/2}$ observed at −0.45 V. Additionally, the one with highest $It^{1/2}$ is with the lowest log t value. The benefit of $It^{1/2}$ vs. log t plots is that the time domains are well evidenced, whereas in I vs. t plot they emerge overlapped.

The current time dependence for the linear diffusion can be represented by the sum of an infinite series of terms depending on the reduced time $t/\tau_{d,}$ where t is the time elapsed from the beginning of the potential step and τ_d is the diffusion constant

$$I_d\,(t) = 2\,(\Delta Q/\pi d) \sum \exp\{-(2n-1)^2\, \pi^2\, t/4\pi d\} \quad (4)$$

(where, n ranges from 1 to ∞)

This expression is related to the cottrell relationship in the short time region ($t<<\tau_d$)

$$I_{Cottrell}(t) = \Delta Q/(\pi/\tau_d)^{1/2} = -(FAD^{1/2}\, \Delta\, c\, /\pi t) \quad (5)$$

and the exponential decay of current with time in the long-time domain ($t>>\tau_d$).

The response of the Gr/GO-SH/AuNs/ChOx electrode towards cholesterol in both the short time region and long-time domain is equivalent and therefore the diffusion coefficient obtained will remain same this is because of the diffusion length 'L'-which is the

characteristic length of the AuNs used to fabricate the biosensor. Therefore D can be calculated from the slope of the linear range in the plot of ln I(t) vs. t [40]. The chemical diffusion coefficient obtained from PITT are plotted as a function of electrode potential in Fig. 6A and the values are as summarized in Table 2. The negative sign in the obtained values may signify higher concentration gradient of H_2O_2 between the bulk and the interface. From the obtained results we conclude that −0.450 V is potential with highest diffusion of cholesterol.

3.7. Influence of pH and temperature on Gr/GO-SH/AuNs/ChOx electrode

The influence of pH of the assay solution over the range 3 to 10 on the amperometric response of the Gr/GO-SH/AuNs/ChOx biosensor towards 3 mM cholesterol was investigated as depicted in Fig. 6B. The variation in pH shows significant effect on the peak current and applied potential. The peak current increased with increase in pH from 3−7 and reached maximum at pH 7. This is in consistence with the pH effects reported for immobilized ChOx [41]. The peak current gradually decreases as the pH increased from 7−10. This signifies that protonation of hydroxyl group in cholesterol takes place at lower pH whereas at higher pH, the electrocatalytic action is more difficult due to the deficiency of protons.

The effect of temperature was scrutinized for the developed cholesterol biosensor. Fig. 6C shows the electrochemical response at different temperatures (10 to 90ºC) in 3 mM cholesterol. A 10 ºC augment in temperature will boost the enzyme activity by 50−100 %. However, the temperature deviation of 2 ºC will result in small increase of 10−20%. As we increased the temperature, the current increased and the optimal catalytic activity of the ensnared ChOx was obtained at 80 ºC. This increased thermal stability at higher temperatures *i.e*. upto 80 ºC is attributed to the AuNs acting as a scaffold providing biocompatibility and thus preventing denaturation of enzyme due to extensive conformational changes. Although the biosensor shows a maximum response at 80 ºC all the experiments were carried out at room temperature to prevent possible solution evaporation and ease of operations. The data obtained was used to construct Arrhenius plot to calculate the activation energy of the ChOx. The Arrhenius equation is as follows [42]

$$I(\mathrm{T}) = I_o \exp\left(E_a / RT\right) \qquad (6)$$

By plotting log I vs. $1/T$ graphs, the activation energy was determined from the slope which was found to be 0.964 kJ/mol. This E_a value is lower than 15.56 kJ/mol and 22.96 kJ/mol for ChOx/AEAPTS/ITO electrode [43] and ChOx/PANI-TX-100 [44] respectively. This smaller E_a indicates that the ChOx immobilized on AuNs/GO-SH modified Gr electrode retains its native structural confirmation which permits easy transfer of electrons from the redox centres of ChOx to the electrode surface and vice versa.

3.8. Chronoamperometric response of the Gr/GO-SH/AuNs/ChOx biosensor

The calibration curve for the detection of cholesterol was acquired by using the Gr/GO-SH/AuNs/ChOx biosensor under optimal conditions [Fig. 7A]. The injection of increasing concentration of cholesterol (0.05 mM to 11.45 mM) resulted in reduction current response experiencing a response time of 4 s; this change is proportional to the concentration of cholesterol. The sensitivity determined was found to be 273 mA/mM/cm^2. The detection limit was determined to be 0.2 nM. The apparent Michaelis-Menten K_M^{app} constant equation which indicates the enzyme substrate kinetics, was determined from the slope of Linewearver Burk plot (inverse of I vs. Inverse of concentration)

$$1/I = K_M^{app}/I_{max} \times 1/C \ + 1/ I_{max} \qquad (7)$$

The K_m value determines the affinity of the enzyme towards its substrate concentration. The smaller K_m specifies higher affinity towards its substrate. The K_m value of the Gr/GO-SH/ AuNs /ChOx biosensor was found to be 0.18 mM which is lower than AuPt–Ch–IL/GCE [45] (0.24 mM) and AgNPs/GCE [46] (1.6 mM). Such a lower K_m value can be attributed to favourable orientation of the ChOx on the biocompatible AuNs that afford high surface coverage area to accommodate more number of enzyme molecules. The efficiency of the Gr/GO-SH/AuNs/ChOx biosensor was analogize to the other modified electrodes reported for the determination of cholesterol and is as shown in Table 3 [45, 47-54]. Our electrode shows superior linear range, good response time with excellent sensitivity and a good detection limit. These extraordinary properties can be attributed to the presence of AuNs. At this point, it is noteworthy to state that the analytical data obtained in the present investigation have been contributed to an improvement in the detection limit of the cholesterol biosensor previously published by our research group [55]

3.9. Selectivity of Gr/GO-SH/AuNs/ChOx biosensor

The accomplishment of the developed Gr/GO-SH/AuNs/ChOx biosensor was tested for its preference of cholesterol in presence of various interferents such as 1 mM AA, 0.05 mM UA and 1 mM acetaminophen. Fig. 7B shows the consequence of interferents on the biosensor in presence of 1 mM cholesterol. The amperometric response of the biosensor towards cholesterol produced an increase in peak current whilst, there was insignificant current change in presence of the interferents. This signifies that Gr/GO-SH/AuNs/ChOx biosensor has the ability to select cholesterol alone in presence of interfering substances. The high selectivity can be accredited to the existence of ChOx layer that selectivity catalyses cholesterol and also to the AuNs that eliminates the necessity for over potential for detection of cholesterol. With this satisfactory selectivity, Gr/GO-SH/AuNs/ChOx biosensor might be applied to the determination of cholesterol in serum or uric samples.

3.10. Repeatability, reproducibility and stability of the Gr/GO-SH/AuNs/ChOx biosensor

The repeatability, reproducibility and stability of the developed biosensor were examined by using CV. The current response of the biosensor in 1 mM cholesterol was noted. The relative standard deviations (RSD) were 8.6% for about 12 successive readings, demonstrating acceptable repeatability of the developed biosensor. In addition, the biosensor exhibited good reproducibility, when estimated in PBS (0.1 M) containing 3 mM cholesterol for five independent electrodes fabricated using the same procedure. The RSD for cholesterol determination at these electrodes was 3.5%. Furthermore, the storage stability of the biosensor was also tested by measuring the current response towards cholesterol. This was repeated twice for about 6 weeks and was kept at 4 ºC when not in use. The current response was about 85-90% its initial value until the 6^{th} week later on which it tends to decrease. The results indicated that Gr/GO-SH/AuNs/ChOx biosensor has excellent repeatability, reproducibility and stability.

3.11 Determination of cholesterol in serum sample using the proposed electrode

For the practical applicability of the developed biosensor, attempts have been made to determine cholesterol using Gr/GO-SH/AuNs/ChOx in serum samples. With this aim, the serum sample was collected from a local Medical Institute and the cholesterol was first determined using the spectrophotometric technique as a reference method as described in the Supplementary information. The concentration of cholesterol was determined from the standard calibration curve and the percentage recovery, relative standard deviation (RSD) was found to be as listed in Table 4. The obtained data were compared with spectrophotometric method and it was observed that the amount of cholesterol found (1.02,

3.12 and 4.76 mM) using Gr/GO-SH/AuNs/ChOx electrode is consistent with the reference method (0.98, 3.21 and 4.73 respectively). Furthermore, paired t test at 95% confidence interval was estimated to statistically compare the data obtained by both the methods. The calculated t value was found to be 0.159 which is smaller than the critical value 2.919 (α=0.05) indicating the proposed electrode is not statistically different from the reference method at 95% confidence interval. These results validate that the proposed electrode can be efficiently used as a reliable electrochemical biosensor for the determination of cholesterol in clinical diagnostics.

4. Conclusion

In conclusion, the present work has employed a new template for the synthesis of AuNs. This is the first report that demonstrates the utility of β-FFNTs as a sacrificial element for the synthesis of 1D nanostructure. We also conclude that the ultrasound irradiation method used for the synthesis of AuNPs is an efficient method for the preparation of uniform and highly dispersive metal nanoparticles. Analytical techniques such as XRD and SEM reveal the face centered cubic, tubular morphology of the AuNs. Surface composition was examined using EDAX. These results demonstrate that the particle size of AuNPs is 14 nm and we succeeded in the synthesis of 1D AuNs. One of the most important aims of the present investigation is to develop a highly sensitive cholesterol biosensor using AuNs. This particular architecture AuNs was chemisorbed on GO-SH modified Gr electrode for the easy fabrication of biosensor. This nanohybrid electrode was characterized using electrochemical techniques like CV, EIS. The resulting biosensor was used for the detection of cholesterol using CV, chronoamperometry under optimum experimental parameters. Based on the electrochemical evaluation, AuNs has been shown to possess high surface to volume ratio, high electron conductivity and promote direct electron transfer between the enzyme and the electrode surface. Analysis of chronoamperometric data illustrates the biosensor has rapid response time, high sensitivity, wide linear range and low detection limit. The investigations of selectivity, operational repeatability, reproducibility and stability have shown satisfactory results. Finally, the proposed electrode has been successfully applied for the determination of cholesterol in serum samples.

Acknowledgements

The authors gratefully acknowledge the financial assistance from the Department of Atomic Energy – Board of Research in Nuclear Sciences, Government of India. We also thank Sri. A.V.S. Murthy, honorary secretary, Rashtreeya Sikshana Samiti Trust, Bangalore and Dr Snehalata Nadiger, Principal, N.M.K.R.V. College for Women, Bangalore for their continuous support and encouragement.

References

[1] S. Aravamudhan, A. Kumar, S. Mohapatra, S. Bhansali, Sensitive Estimation of Total Cholesterol In Blood Using Au Nanowires Based Micro-Fluidic Platform, Biosens. Bioelectron. 22 (2007) 2289–2294.

[2] A. Ahmadalinezhad, A. Chen, High-Performance Electrochemical Biosensor for the Detection of Total Cholesterol, Biosens. Bioelectron. 26 (2011) 4508–4513.

[3] M.B. Gholivand, M. Khodadadian, Amperometric Cholesterol Biosensor Based on the Direct Electrochemistry of Cholesterol Oxidase and Catalase on A Graphene/Ionic Liquid-Modified Glassy Carbon Electrode, Biosens. Bioelectron. 53 (2014) 472–478.

[4] J. MacLachlan, A.T.L. Wotherspoon, R.O.Ansell, C.J.W. Brooks, Cholesterol Oxidase: Sources, Physical Properties and Analytical Applications, J. Steroid Biochem. Mol. Biol. 72 (2000) 169−195.

[5] D. J. Sellmyer, M. Yu, R. D. Kirby, Nanostructured magnetic films for extremely high density recording, Nanostruct. Mater. 12 (1999) 1021−1026.

[6] U. Kreibig, H. Bonnemann, J. Hormes, Nanostructured Metal Clusters and Colloids, in: H. S. Nalwa (Eds.), Handbook of surfaces and interfaces of materials, Academic press, San Diego, 2001, pp. 1−85

[7] D.W. Bahnemann, Ultrasmall Metal Oxide Particles: Preparation, Photophysical Characterization and Photocatalytic Properties, Israel J. Chem. 33 (1993) 115−136.

[8] Q. Li, H. Li, V.G. Pol, I. Bruckental, Y. Koltypin, J. Calderon-Mereno, I. Nowik, A. Gedanken, Sonochemical synthesis, structural and magnetic properties of air-stable Fe/Co alloy nanoparticles, New J. Chem. 27 (2003) 1194−1199.

[9] Y. Wang, X. Jiang, Y. Xia, A Solution-Phase, Precursor Route to Polycrystalline SnO_2 Nanowires that can be used for Gas Sensing under Ambient Conditions, J. Am. Chem. Soc. 125 (2003) 16176–16177.

[10] Z. W. Pan, Z. R. Dai, Z. L. Wang, Nanobelts of Semiconducting Oxides, Science 291 (2001) 1947–1949.

[11] G. K. Mor, K. Shankar, M. Paulose, O. K. Varghese, C. A. Grimes, Use of Highly-Ordered TiO_2 Nanotube Arrays in Dye-Sensitized Solar Cells, Nano Lett. 6 (2006) 215–218.

[12] G. Z. Shen, Y. Bando, C. H. Ye, X. L. Yuan, T. Sekiguchi, D. Golberg, Single-Crystal Nanotubes of II_3–V_2 Semiconductors, Angew. Chem. Int. Ed. 45 (2006) 7568−7572.

[13] K. Pelzer, K. Philippot, B. Chaudret, W. Meyer-Zaika, G. Schmid, Ruthenium Nanoparticles in Nanoporous Alumina Membranes: Preparation, Characterization and Catalytic Properties, Z. Anorg. Allg. Chem. 629 (2003) 1217−1222.

[14] K. Kordas, G. Toth, J. Levoska, M. Huuhtanen, R. Keiski, M. Harkonen, T. F George, J. Vahakangas, Room Temperature Chemical Deposition of Palladium Nanoparticles In Anodic Aluminium Oxide Templates, Nanotechnology 17 (2006) 1459−1463.

[15] J. G. Heddle, Gold Nanoparticle-Biological Molecule Interactions and Catalysis, Catalysts 3 (2013) 683−708.

[16] S. Eliyahu, A. Vaskevich, I. Rubinstein, On the formation mechanism of metal nanoparticle nanotubes, Thin Solid Films 518 (2010) 1661−1666.

[17] M. Spuch-Calvar, J. Pacifico, J. Perez-Juste, L. M. Liz-Marzan, Synthesis and Optical Characterization of Submicrometer Gold Nanotubes Grown on Goethite Rods, Langmuir 24 (2008) 9675−9681.

[18] Y. Qu, R. Porter, F. Shan, J. D. Carter, T. Guo, Synthesis of Tubular Gold and Silver Nanoshells Using Silica Nanowire Core Templates, Langmuir 22 (2006) 6367−6374.

[19] M. Reches, E. Gazit, Casting Metal Nanowires within Discrete Self-Assembled Peptide Nanotubes, Science 300 (2003) 625−627.

[20] S. Guha, A. Banerjee, Self-Assembled Robust Dipeptide Nanotubes and Fabrication of

Dipeptide-Capped Gold Nanoparticles on the Surface of these Nanotubes, Adv. Funct. Mater. 19 (2009) 1949−1961

[21] R. Djalali, Y.F. Chen, H. Matsui, Au Nanocrystal Growth on Nanotubes Controlled by Conformations and Charges of Sequenced Peptide Templates, J. Am. Chem. Soc. 125 (2003) 5873−5879.

[22] K. Lu, V.P. Conticello, D.G. Lynn, Templating Colloidal Metal Nanoparticle Assemblies: Use of the Aβ Amyloid Peptide Nanotube, Mater. Res. Soc. Symp. Proc. 826E, Warrendale, PA, 2004.

[23] Y. Song, S.R. Challa, C.J. Medforth, Y. Qiu, R.K. Watt, D. Pena, J.E. Miller, F.V. Swol, J.A. Shelnutt, Synthesis of Peptide-Nanotube Platinum-Nanoparticle Composites, Chem. Commun. (2004) 1044−1045.

[24] B. Peng, M. Locascio, P. Zapol, S. Li, S.L. Mielke, G.C. Schatz, H.D. Espinosa, Measurements of Near-Ultimate Strength For Multiwalled Carbon Nanotubes and Irradiation-Induced Crosslinking Improvements, Nat. Nanotechnol. 3 (2008) 626−631.

[25] K. H. Anderson, The Synthesis and Surface Studies of β-Amino Acids and β-Peptides Ph.D. Thesis, University of Canterbury, 2007.

[26] S. Min, X. Juan, W. Changzi, The effect of surface functionalization on the immobilization of gold nanoparticles on graphene sheets, J. Nanotechnol. (2012) DOI: 10.1155/2012/329318.

[27] J. Li, Y. Sha, A convenient synthesis of amino acid methyl ester, Molecules 13 (2008) 1111−1119.

[28] D. Seebach, M. Overhand, F.N.M. Kiihnle, B. Martinoni, L. Oberer, U. Hommel, H. Widmer, β-Peptides: Synthesis by Arndt-Eistert Homologation with Concomitant Peptide Coupling, Hel. Chim. Acta 79 (1996) 913−941.

[29] J.H. Kim, M. Lee, J.S. Lee, C.B. Park, Self-Assembled Light-Harvesting Peptide Nanotubes for Mimicking Natural Photosynthesis, Angew. Chem. Int. Ed. 51 (2012) 517−520.

[30] J. Debgupta, V. K. Pillai, Thiolated Graphene–A New Platform for Anchoring CdSe Quantum Dots for Hybrid Heterostructures, Nanoscale 5 (2013) 3615–3619.

[31] B. Huang, N. Jia, L. Chen, L. Tan, S. Yao, Electrochemical Impedance Spectroscopy Study on Polymerization of l-Lysine on Electrode Surface and Its Application for Immobilization and Detection of Suspension Cells, Anal. Chem. 86 (2014) 6940−6947.

[32] A. P. Kujundziski, D. Chamovska, T. Grchev, Capacitive properties of polypyrrole/activated carbon composite, Hem. Ind. 68 (2014) 709−719.

[33] A.A. Abdelwahab, M.S. Won, Y.B. Shim, Direct Electrochemistry of Cholesterol Oxidase Immobilized on a Conducting Polymer: Application for a Cholesterol Biosensor, Electroanalysis 22 (2010) 21−25.

[34] J.E. Frew, H.A.O. Hill, Direct and Indirect Electron Transfer between Electrodes and Redox Proteins, Eur. J. Biochem. 172 (1988) 261−269.

[35] A.M.C.F. Oliverua Brett, M.H. Gill, A.P. Piedade, An Electrochemical Bienzyme Membrane Sensor for Free Cholesterol, Bioelectrochem. Bioenerg. 28 (1992) 105−115.

[36] E. Laviron, General Expression of the Linear Potential Sweep Voltammogram In the Case of Diffusionless Electrochemical Systems, J. Electroanal. Chem. 101 (1979) 19−28.

[37] J.Y. Yang, Y. Li, S.M. Chen, K.C. Lin, Fabrication of a Cholesterol Biosensor Based on Cholesterol Oxidase and Multiwall Carbon Nanotube Hybrid Composites, Int. J. Electrochem. Sci. 6 (2011) 2223–2234.

[38] J. Li, F. Yang, X.X. Mark, W. Verbrugge, Y.T. Cheng, Potentiostatic Intermittent Titration Technique (PITT) For Spherical Particles with Finite Interfacial Kinetics, Electrochim. Acta 75 (2012) 56–61.

[39] H. Manjunatha, T.V. Venkatesha, G.S. Suresh, Kinetics of Electrochemical Insertion of Lithium Ion Into Lifepo$_4$ From Aqueous 2 M Li_2SO_4 Solution Studied By Potentiostatic Intermittent Titration Technique, Electrochim. Acta 58 (2011) 247–257.
[40] H. Xia, L. Lu, G. Ceder, Li Diffusion in LicoO_2 Thin Films Prepared By Pulsed Laser Deposition, J. Power Sources 159 (2006) 1422–1427.
[41] C. Zhao, L. Wan, L. Jiang, Q. Wang, K. Jiao, Highly sensitive and selective cholesterol biosensor based on direct electron transfer of haemoglobin, Anal. Biochem. 383 (2008) 25–30.
[42] H.B. Yildiz, D.O. Demirkol, S. Sayin, M. Yilmaz, O. Koysuren, M. Kamaci, New Amperometric Cholesterol Biosensors Using Poly(ethyleneoxide) Conducting Polymers, J. Macromol. Sci. Part A-Pure Appl. Chem. 50 (2013) 1075−1084.
[43] S.K. Arya, A.K. Prusty, S.P. Singh, P.R. Solanki, M.K. Pandey, M. Datta, Cholesterol biosensor based on N-(2-aminoethyl)-3-aminopropyl-trimethoxysilane self-assembled monolayer, Anal. Biochem. 363 (2007) 210–218.
[44] R. Khan, P.R. Solanki, A. Kaushik, S.P. Singh, S. Ahmad, B.D. Malhotra, Cholesterol biosensor based on electrochemically prepared polyaniline conducting polymer film in presence of a nonionic surfactant, J. Polym. Res.16 (2009) 363–373.
[45] A. Safavi, F. Farjami, Electrodeposition of Gold–Platinum Alloy Nanoparticles on Ionic Liquid–Chitosan Composite Film and Its Application in Fabricating an Amperometric Cholesterol Biosensor, Biosens. Bioelectron. 26 (2011) 2547–2552.
[46] S. Nantapol, O. Chailapakul, W. Siangproh, Sensitive and selective electrochemical sensor using silver nanoparticles modified glassy carbon electrode for determination of cholesterol in bovine serum, Sens. Actuators B 207 (2015) 193−198.
[47] S.S.J. Aravind, T.T. Baby, T. Arockiadoss, R.B. Rakhi, S. Ramaprabhu, A Cholesterol Biosensor Based on Gold Nanoparticles Decorated Functionalized Graphene Nanoplatelets, Thin Solid Films 519 (2011) 5667−5672.
[48] U. Saxena, M. Chakraborty, P. Goswami, Covalent Immobilization of Cholesterol Oxidase on Self-Assembled Gold Nanoparticles For Highly Sensitive Amperometric Detection of Cholesterol in Real Samples, Biosens. Bioelectron. 26 (2011) 3037–3043.
[49] P. Gomathi, D. Ragupathy, J.H. Choi, J.H. Yeum, S.C. Lee, J.C. Kim, S.H. Lee, H.D. Ghima, Fabrication of Novel Chitosan Nanofiber/Gold Nanoparticles Composite Towards Improved Performance For a Cholesterol Sensor, Sens. Actuators B, 153 (2011) 44–49.
[50] M. Eguílaz, R. Villalonga, L. Agüí, P. Yáñez-Sedeño, J.M. Pingarrón, Gold Nanoparticles: Poly(Diallyldimethylammonium Chloride)–Carbon Nanotubes Composites as Platforms for the Preparation of Electrochemical Enzyme Biosensors: Application to the Determination of Cholesterol, J. Electroanal. Chem. 661 (2011) 171–178
[51] G.P.Nikoleli, Z.H. Ibupoto, D.P. Nikolelis, V. Likodimos, N. Psaroudakis, N.Tzamtzis, M. Willander, T. Hianik, Potentiometric cholesterol biosensing application of graphene electrode with stabilized polymeric lipid membrane, Cent. Eur. J. Chem. 11 (2013) 1554–1561.
[52] V. N. Psychoyios, G.P. Nikoleli, N. Tzamtzis, D. P. Nikolelis, N. Psaroudakis, B. Danielsson, M. Q. Israr, M. Willandere, Potentiometric Cholesterol Biosensor Based on ZnO Nanowalls and Stabilized Polymerized Lipid Film, Electroanal. 25 (2013) 367–372.
[53] Z.H. Ibupoto, S. Elhag, O. Nur, M. Willander, Fabrication of Sensitive Potentiometric Cholesterol Biosensor Based on Co_3O_4 Interconnected Nanowires, Electroanal. 26 (2014) 1928–1934.
[54] Z.H. Ibupoto, K. Khun, X. Liu, M. Willander, Low temperature synthesis of seed

mediated CuO bundle of nanowires, their structural characterization and cholesterol detection, Mater. Sci. Eng. C, 33 (2013) 3883–3898.
[55] R. Manjunatha, D.H. Nagaraju, G.S. Suresh, J.S. Melo, S.F. DSouza, T.V. Venkatesha, Direct electrochemistry of cholesterol oxidase on MWCNTs, J. Electroanal. Chem. 651 (2011) 24–29.

Figure Captions

Scheme-1 Schematic view of the fabrication processes of the cholesterol biosensor

Fig. 1 XRD patterns of the as synthesized (A) AuNPs, (B) self assembled β-FFNTs and (C) AuNPs templated peptide nanotubes. The symmetry of the structures is shown by the peaks labelled △= 10.03°, 18.3°, 19.6° for peptides and ○= 38.1°, 44.4° and 64.6° for Au respectively.

Fig. 2 SEM of (A) AuNPs and (B) corresponding histograms of AuNPs synthesized by ultrasound irradiation, peptide nanotubes self assembled at different dilution (C) 2 mg/mL and (D) 1 mg/mL, (E) AuNPs ensembled peptide nanotubes and (f) AuNs obtained after peptide cleavage.

Fig. 3 (A) Cyclic voltamograms of (a) bare Gr (b) Gr/GO-SH (c) Gr/GO-SH/AuNs (d) Gr/GO-SH/AuNs/ChOx in 5 mM $Fe(CN)_6^{3-/4-}$ solution. (B) Nyquist diagrams of (a) bare Gr (b) Gr/GO-SH (c) Gr/GO-SH/AuNs (d) Gr/GO-SH/AuNs/ChOx. Inset displays the equivalent circuit compatible with the experimental data

Fig. 4 CVs of 0.3 mM cholesterol at (a) Gr/ChOx (b) Gr/GO-SH/ChOx (c) Gr/GO-SH/AuNs (d) Gr/GO-SH/AuNs/ChOx in oxygen saturated 0.1 M PBS with the scan rate of 50 mV/s. Inset is the comparative CV of (a') Gr/GO-SH/AuNPs with (b') Gr/GO-SH/AuNs.

Fig. 5 (A) CV responses of Gr/GO-SH/AuNs/ChOx electrode for different concentrations (0 to 6 mM) of cholesterol in 0.1 M oxygen saturated PBS solution. Inset is the plot of peak current against added cholesterol concentration (R= 0.9886). (B) CVs of 2 mM cholesterol at the Gr/GO-SH/AuNs/ChOx electrode at different scan rates (a-l: 10 to 100 mV/s). Inset is the dependence of the anodic and cathodic peak current on the scan rate.

Fig. 6 (A) Dependence of chemical diffusion coefficient of Gr/GO-SH/AuNs/ChOx electrode at different potential. Inset $It^{1/2}$ vs. log t plot for the proposed biosensor. (B) Dependence of cathodic peak currents of 3 mM cholesterol on pH values (3 to 10) of the solution at Gr/GO-SH/AuNs/ChOx electrode (C) Effect of temperature on the CV response of the modified electrode to 3 mM cholesterol. Inset- Line weaver Burk plot of $1/I$ vs. 1/cholesterol of Gr/GO-SH/AuNs/ChOx electrode

Fig. 7 (A) Typical amperometric current response of the Gr/GO-SH/AuNs/ChOx electrode upon successive addition of various concentration of cholesterol at an applied potential of –450 mV (vs. SCE) in 0.1 M PBS solution. Inset is the calibration plot of current versus cholesterol concentration. (B) The amperometric response of the modified bioelectrode to successive additions of 1 mM cholesterol and interferences 1 mM AA (b), 0.5 mM UA (c) and 1 mM ACT (d) in 0.1 PBS at pH 7 and an applied potential of –450 mV vs. SCE.

Vitae

S Nandini obtained her B.Sc degree at Bangalore Univeristy in 2008. She received her M.Sc. degree in Biochemistry from Bangalore University, India in 2010. At present she is pursuing Ph.D. at Department of PG Studies and Research in Biochemistry, Kuvempu University in the field of chemical and biochemical sensors. She is a Senior Research Fellow for a DAE–BRNS sponsored research project at Department of Chemistry, NMKRV College for Women, Bangalore, India.

S. Nalini obtained her B.Sc degree at Bangalore University in 2008. She received her M.Sc. degree in Biochemistry from Bangalore University, India in 2010. At present she is pursuing Ph.D. at Department of PG Studies and Research in Biochemistry, Kuvempu University in the field of chemical and biochemical sensors. She is a visiting researcher at Department of Chemistry, NMKRV College for Women, Bangalore, India.

Dr. M. B Madhusudana Reddy, is an Assistant Professor of Chemistry in School of Chemical Sciences at REVA University, Bangalore, India. He received his M. Sc., Chemistry from the Bangalore University in the year 2003 and Ph. D. for the "Synthesis of biologically important compounds in organic chemistry" from Bangalore University in 2012. He did his Post-doctoral studies on design, synthesis and conformation of hybrid peptides at Indian Institute of Science, Bangalore, India.

Dr. G.S. Suresh received his M.Sc. in Chemistry in 1987 and M.Phil. in physical chemistry in 1998 from Bangalore University, India. He received his Ph.D. in chemistry from S.K. University in 2002. He worked with Prof. D. Aurbach, Bar-ilan University, Israel, during 2005–07 and with Prof. S. Sampath, Indian Institute of Science, Bangalore during 2002–03 for his postdoctoral research work. He worked as associate professor at S.S.M.R.V. Degree College 1989-2012. Currently he is working as an associate professor in Chemistry at NMKRV College for Women, since 2011. He is the Principal Investigator for DAE-BRNS, DST and VGST Projects.

Dr. J.S. Melo obtained his M.Sc. in Biochemistry in 1984 and Ph.D. degree in Biochemistry in 1990 from Mumbai University. Currently he is a senior scientific officer of the Nuclear Agriculture & Biotechnology Division at Bhabha Atomic Research Centre, Mumbai, India, and is also an Assistant Professor at the Homi Bhabha National Institute. In the field of bioprocessing, he has developed a number of novel techniques for immobilization of enzymes, cells and preparation of coimmobilizates. His current field of interest is in bioremediation, nanoscience and sensors. He has to his credit several publications in International Journals, Symposiums and Workshops.

Dr. P. Niranjana is currently working as Assistant Professor at Kuvempu University, Shimoga, Karnataka, India. He has obtained M.Sc. and Ph.D. in Biochemistry from Kuvempu University. His area of research includes, development of biosensors, synthesis of nanomaterials, Insect biology etc.

Jakkid Sanetuntikul graduated in Chemical Engineering from Chulalongkorn University, Thailand and he received his M.S. degree in Chemical Engineering from Prince of Songkla University, Thailand. Since March 2011, he is working in Advanced Materials Energy Laboratory for his PhD degree at Daegu Gyeongbuk Institute of Science, South Korea.

Dr. Sangaraju Shanmugam obtained his doctorate in 2004 from Indian Institute of Technology, Madras, India. In 2005, he joined Department of Chemistry, Bar-Ilan University, Israel as a Postdoctoral Fellow. In 2007, he joined as a JSPS postdoctoral fellow at Waseda University. In 2011, he was appointed as an Assistant Professor at DGIST, Korea. Shanmugam currently has 62 referred publications, 5 Indian Patents and filed 4 Korean patents. His technical contributions have been recognized by many awards including JSPS Fellow from Japan, Samuel and Helene Soref Young Scientist from Bar-Ilan University, Israel and Prof. Langmuir Prize for Best Thesis, IIT Madras.

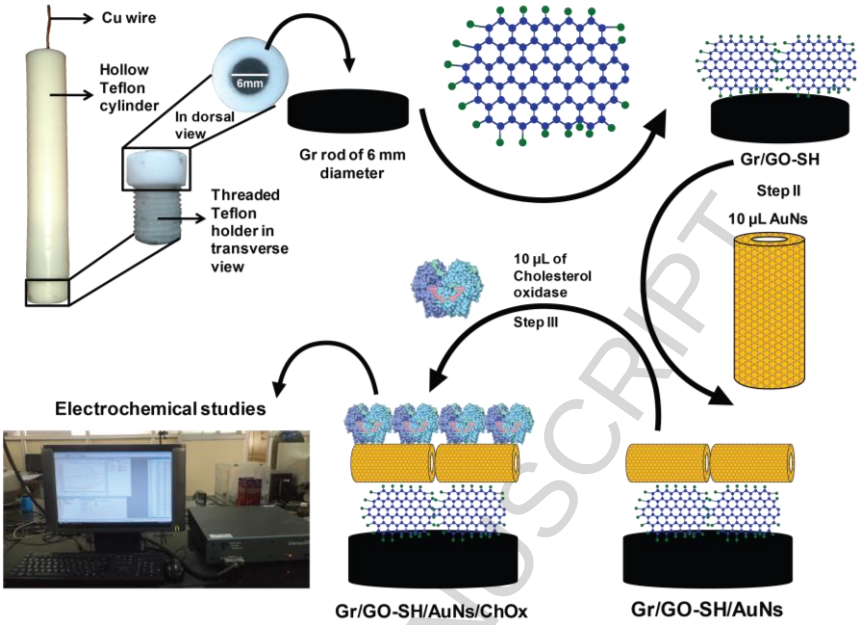

Color in online version only

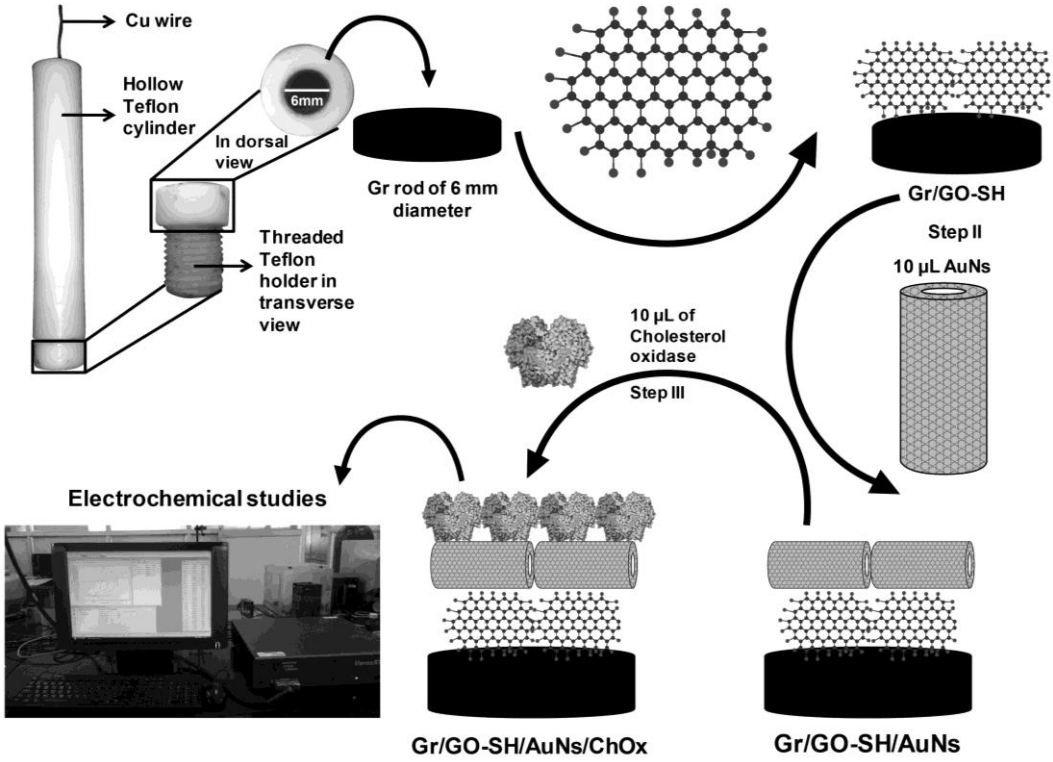

Scheme 1

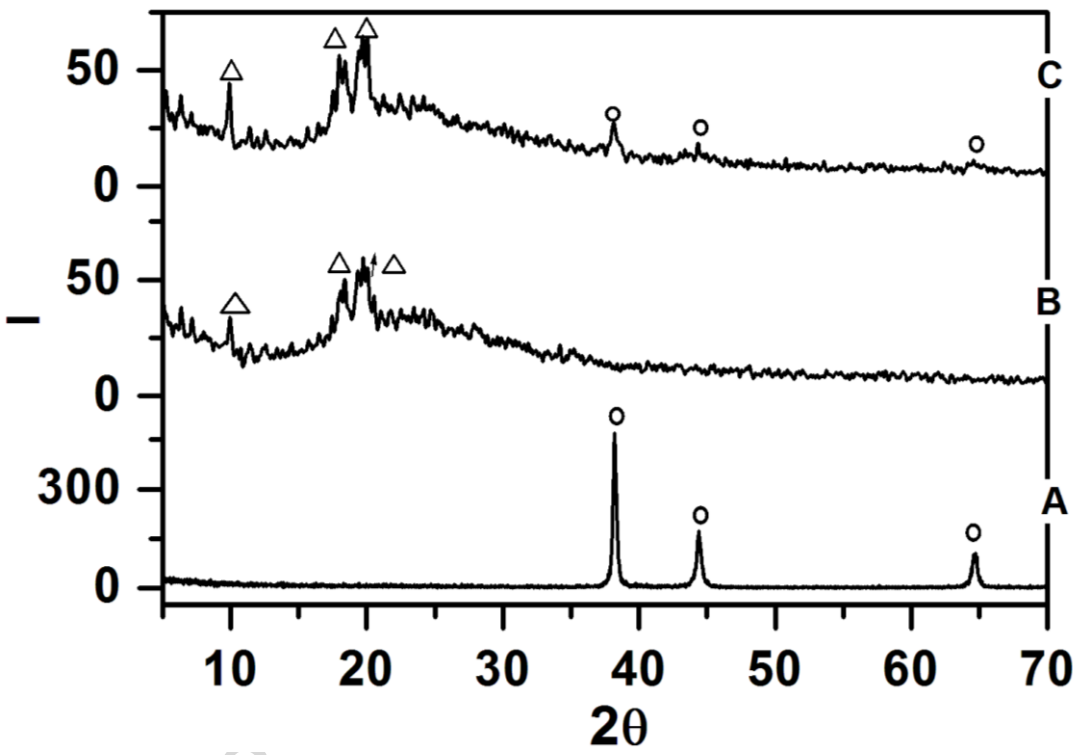

Fig. 1

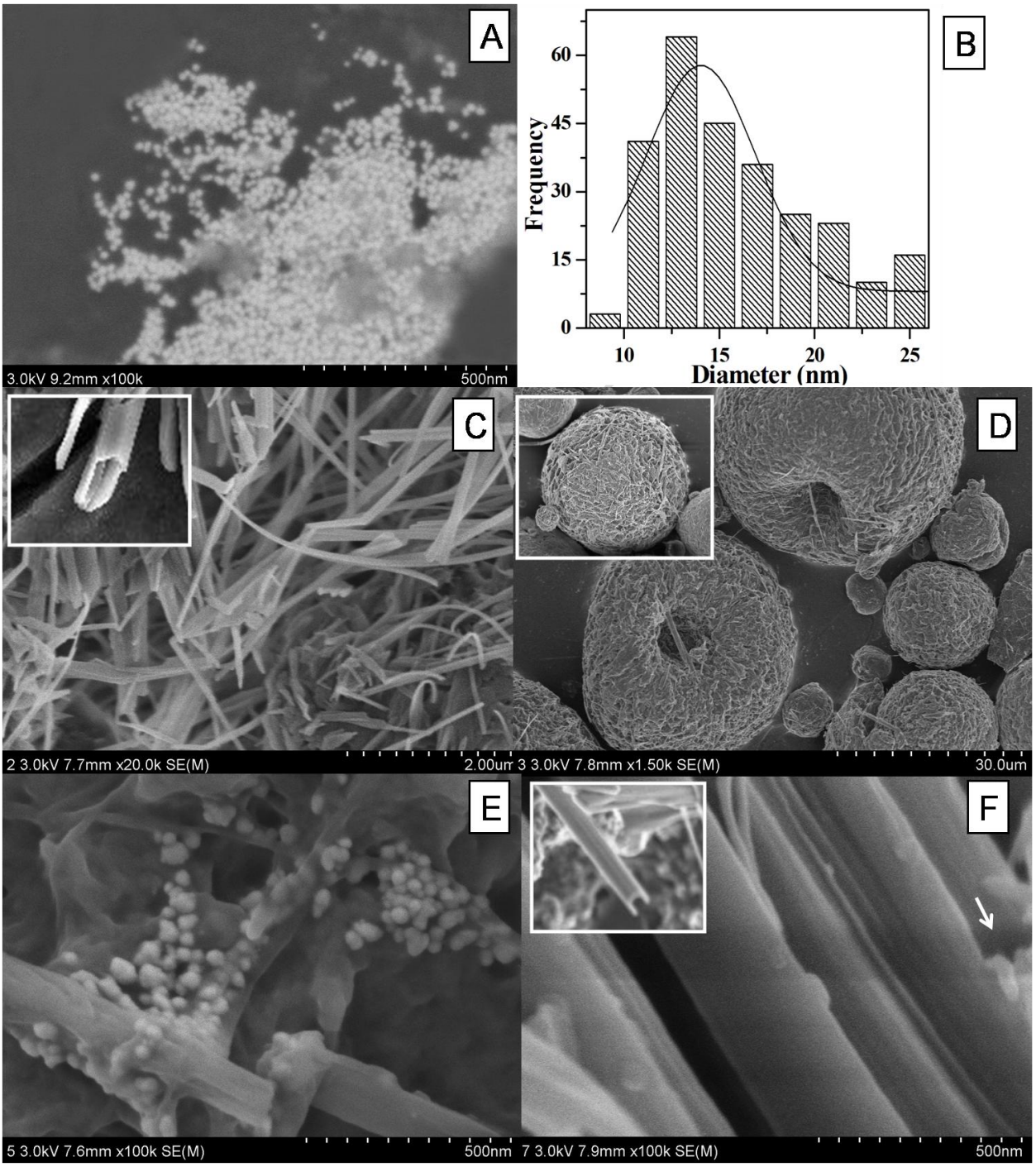
A
3.0kV 9.2mm x100k
500nm
B
Frequency
Diameter (nm)
0
15
30
45
60
10
15
20
25
C
2 3.0kV 7.7mm x20.0k SE(M)
2.00um
D
3 3.0kV 7.8mm x1.50k SE(M)
30.0um
E
5 3.0kV 7.6mm x100k SE(M)
500nm
F
7 3.0kV 7.9mm x100k SE(M)
500nm

Fig. 2

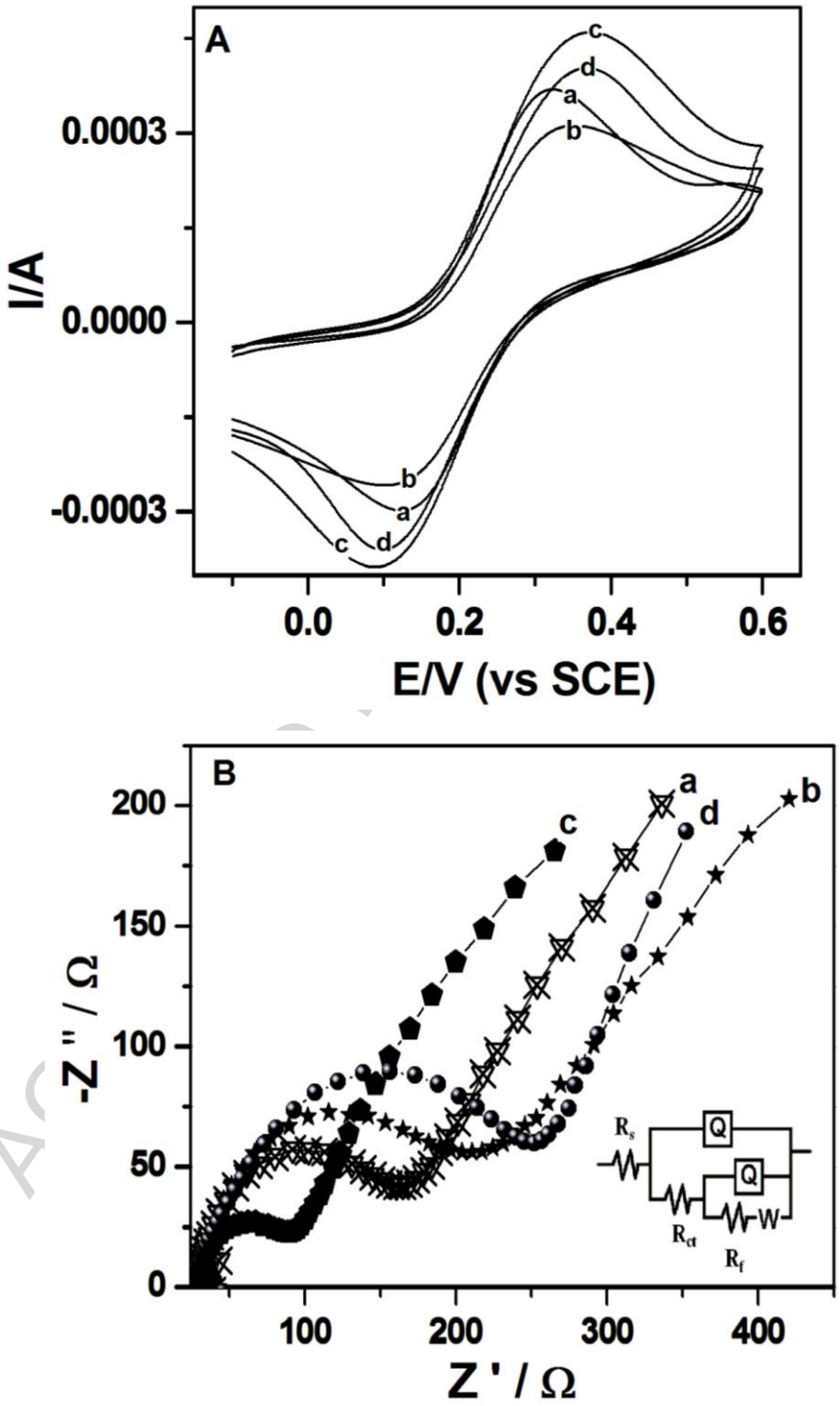

Fig. 3

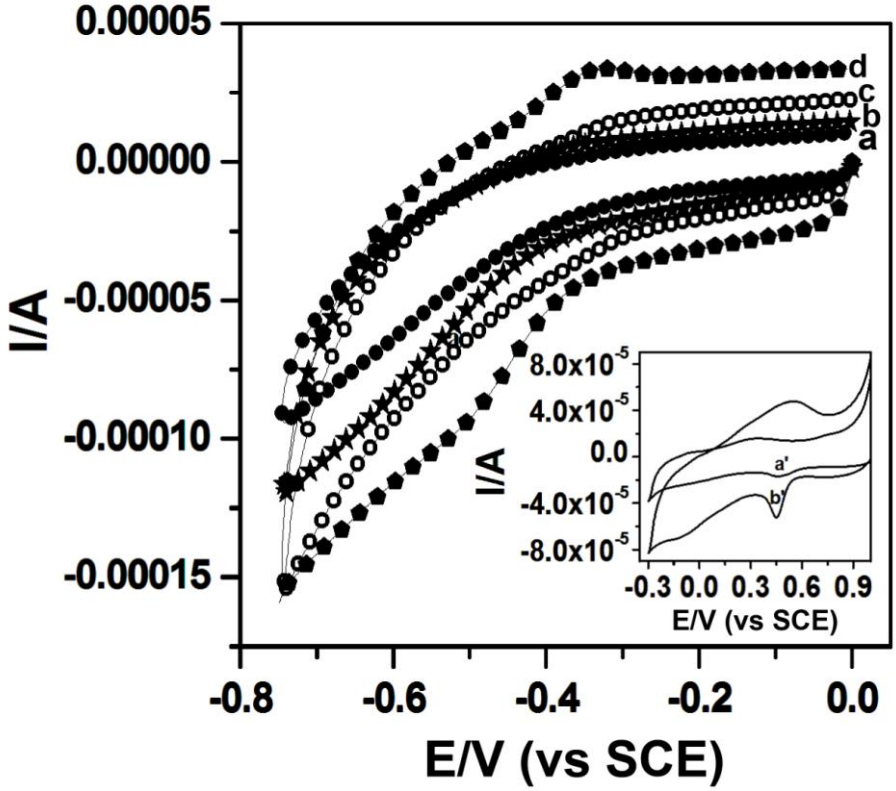

Fig. 4

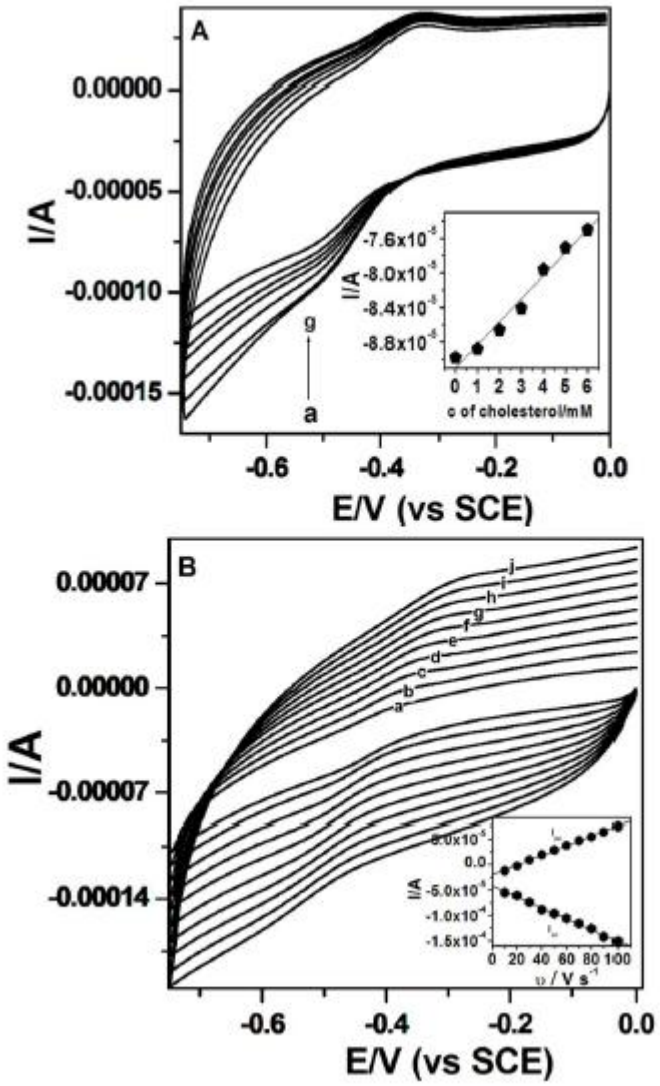

Fig. 5

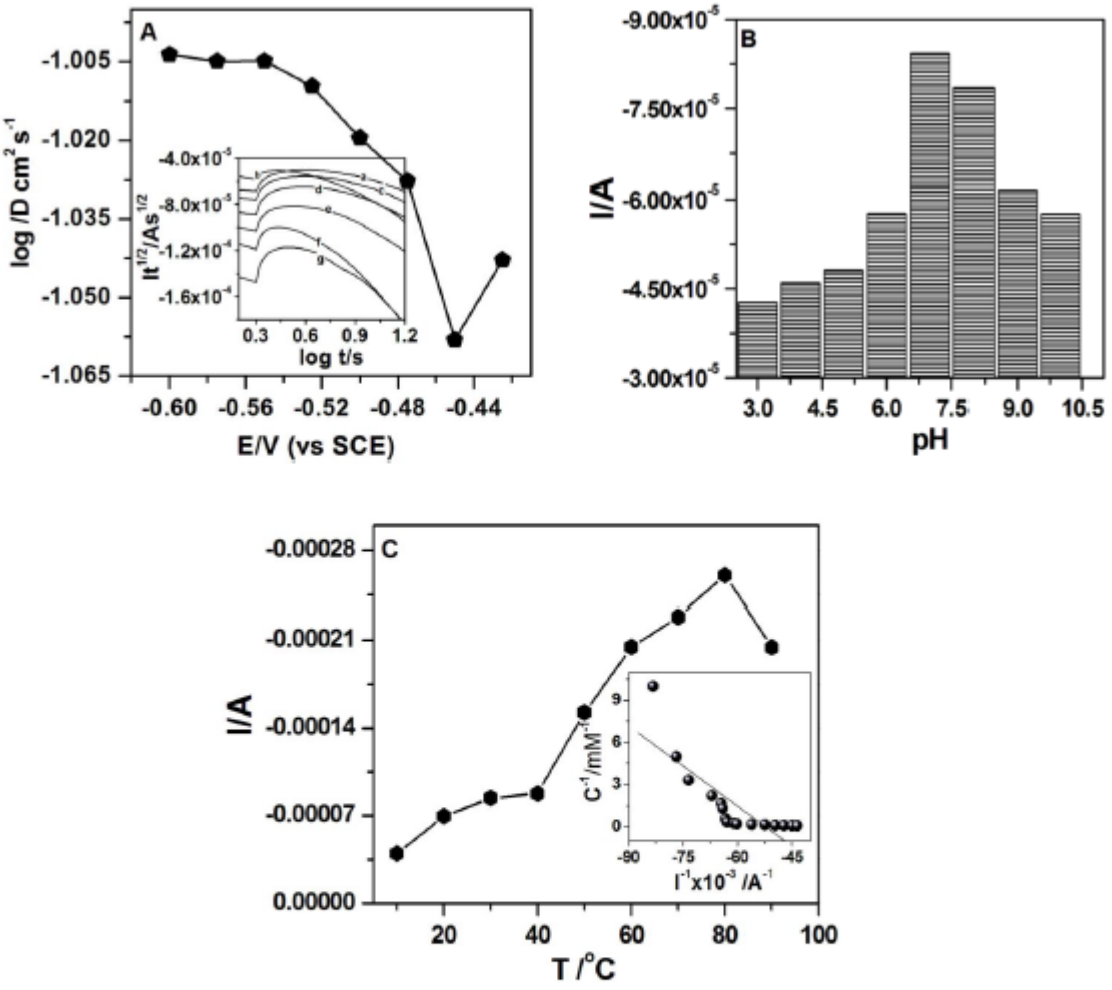

Fig. 6

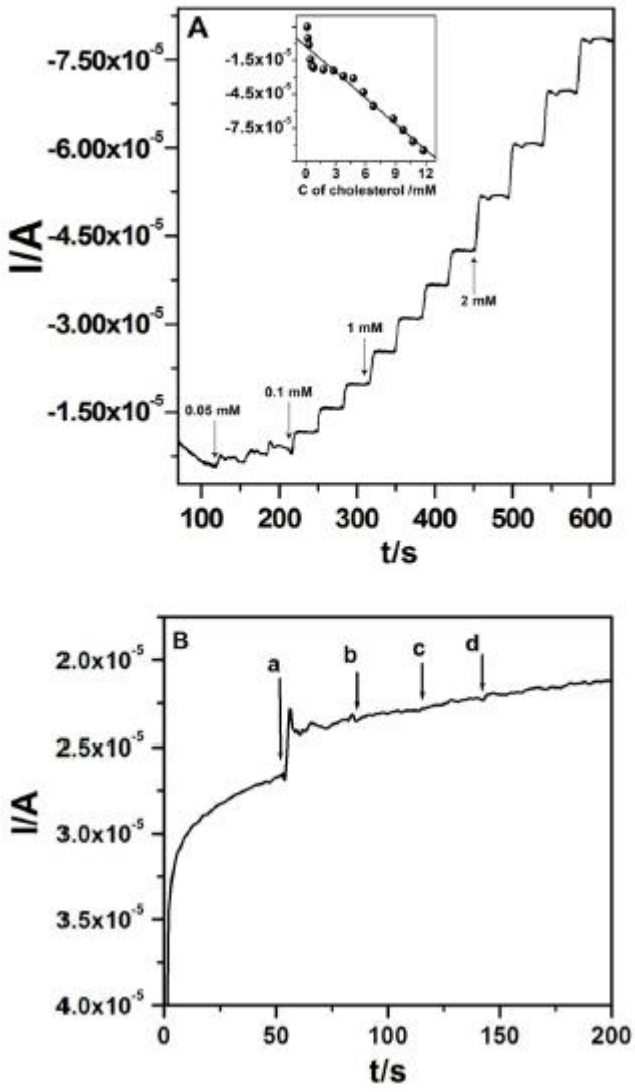

Fig. 7

Passport-type photograph of Authors

S. Nandini Reddy

S. Nalini

Dr. M.B.M.

Dr.G.S.Suresh Niranjana

Dr.J.S.Melo

Dr. P.

J. Sanetuntikul

Dr. S. Shanmugam

Table 1. Impedance components for the Gr/GO-SH/AuNs/ChOx electrodes determined by fitting EIS experimental data using the equivalent circuit

Name of the electrode	R_s (Ω)	Q_1 (m*F*/cm^2)	*n*1	R_f (Ω)	Q_2 (m*F*/cm^2)	*n*2	R_{ct} (Ω)	*W* (Ω)
Gr	124.1	4.87E-2	0.9	238.9	4.53	0.5	30.88	4.69
Gr/GO-SH	34.15	1.40E-2	1	115.2	0.31	0.5	74.68	0.0039
Gr/GO-SH/AuNs	28.97	7.02E-2	0.8	927.7	4.36	0.6	61.63	0.02904
Gr/GO-SH/AuNs/ChOx	27.95	4.7	0.9	252.3	0.16	0.7	85	0.003829

Gr: Graphite; GO-SH: thiol-functionalized graphene oxide; AuNs: gold nanostructure and ChOx: Cholesterol oxidase.

Table 2. Diffusion co-efficient calculated using PITT at different applied potential

Potential Applied (mV)	Diffusion co-efficient (cm^2/s)
–0.425	–1.042
–0.450	–1.058
–0.475	–1.027
–0.500	–1.019
–0.525	–1.009
–0.550	–1.004
–0.575	–1.0049
–0.600	–1.003

Table 3. Comparison of the beneficial analytical data obtained by the proposed with other electrochemical cholesterol sensors

Modified electrode	Linear range (mM)	Response time (s)	Detection limit (nM)	Sensitivity ($mA/mM/cm^2$)	Reference
ChOx/AuPt–Ch–IL/GCE	0.05-6.2 6.2-11.2	7	10000	0.0907	45
Au/f-G modified GCE	0-0.135	–	–	0.000314	47
AuE/dithiol/AuNPs/MUA	0.04-0.2	–	34600	0.00902	48
CSNF–AuNPs/ChOx	0.01-0.045	~5	–	0.00102	49
ChOx/HRP/AuNPs/PDDA / MWCNTs/GCE	0.02–1.2	–	4400	0.0186	50
ChOx/AuNPs/PDDA/ MWCNTs/GCE	0.01–1.05	–	2200	0.00223	50
Other nanostructures	**Linear range (mM)**	**Response time (s)**	**Detection limit (nM)**	**Sensitivity mV/decade**	**Reference**
polymeric lipid enzyme based sensor	-	~5	100	~64	51
ZnO-nanowalls/ ChOx	0.001-1	-	400	~57	52
ChOx/Co_3O_4 nanowires /Au	0.0001-1	10	0.0003	−94	53
CuO nanostructures/ ChOx	0.005-5	10	1000	33.88 ± 0.96	54
Gr/GO-SH/AuNs/ChOx	0.05-11.45	4	0.2	273 $mA/mM/cm^2$	This work

ChOx: Cholesterol oxidase; Au-Pt: gold-platinum; Ch: Chitosan; IL-ionic liquid; GCE: Glassy carbon electrode; f-G: functionalized graphene; AuE: gold electrode; MUA:11-mercaptoundecanoic acid; CSNF:Chitosan nanofiber; AuNPs: gold nanoparticles; HRP: horseradish peroxidase; PDDA: Poly(Diallyldimethylammonium Chloride); MWCNTs: multiwalled carbon nanotubes; ZnO: Zinc oxide; Co3O4: Cobalt oxide; CuO- Copper oxide; Gr: Graphite; GO-SH: thiol-functionalized graphene oxide; AuNs: gold nanostructure and ChOx: Cholesterol oxidase

Table 4 Determination of cholesterol in serum samples (n=5) obtained at Gr/GO-SH/AuNs/ChOx biosensor

Sample No	Added (mM L^{-1})	Found (mM L^{-1}) with 95% confidence interval estimate	Recovery (%) with 95% confidence interval estimate	RSD (%)
1	1	1.02 ±0.09	102±3.8	2.21
2	3	3.12 ±0.15	104±2.5	3.5
3	5	4.76 ± 0.22	95±0.72	5.2

Graphical Abstract

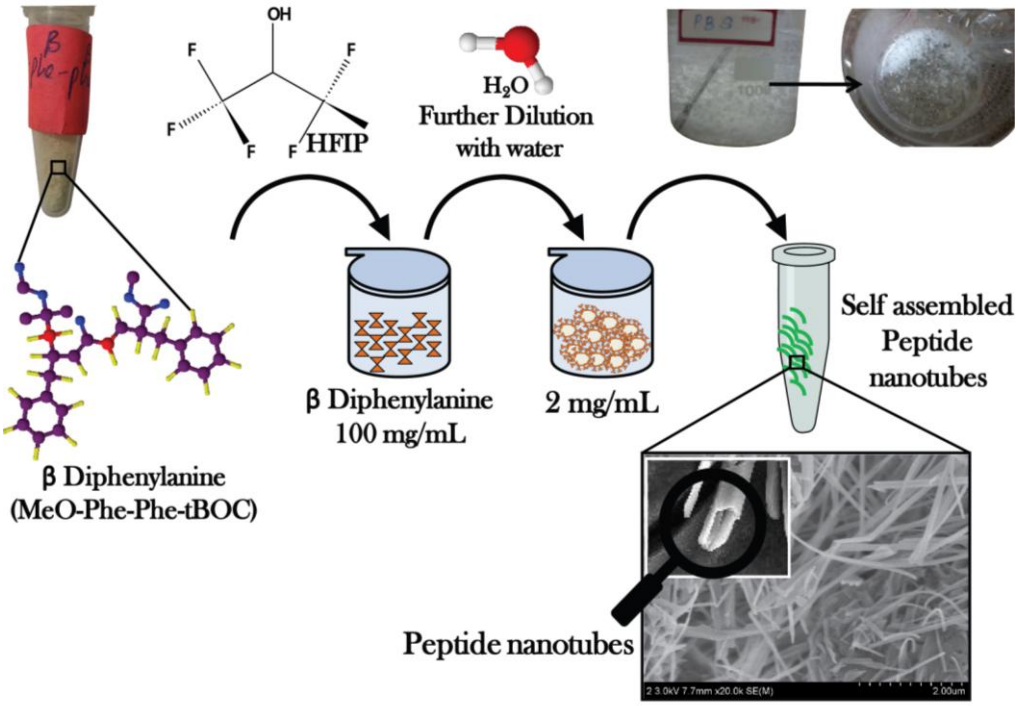

Color in oneline version only

Research Highlights

- The present work has employed a new template (β-FFNTs) for the synthesis of AuNs.
- AuNs was chemisorbed on GO-SH for the fabrication of cholesterol biosensor
- The nanohybrid composite offers enhanced enzyme loading and high sensitivity
- The biosensor shows rapid response time, high sensitivity and low detection limit
- The proposed biosensor has excellent repeatability, reproducibility and stability